An experimental investigation of the steady separated flow past a circular cylinder

By A. S. GROVE,* F. H. SHAIR,† E. E. PETERSEN AND ANDREAS ACRIVOS‡

Department of Chemical Engineering, University of California, Berkeley 4, California

(Received 24 June 1963)

The steady separated flow past a circular cylinder was investigated experimentally. By artificially stabilizing the steady wake, this system was studied up to Reynolds numbers R considerably larger than any previously attained, thus providing a much clearer insight into the asymptotic character of such flows at high Reynolds numbers. Some of the experimental results were unexpected. It was found that the pressure coefficient at the rear of the cylinder remained unchanged for $25 \leqslant R \leqslant 177$, that the circulation velocity within the wake approached a non-zero limit as the Reynolds number increased, and that the wake length increased in direct proportion to the Reynolds number.

1. Introduction

The streaming motion of fluids past arbitrary slender objects is a phenomenon which is, by now, well understood. Many books and literally thousands of articles have been written on the subject, and many methods have been developed, exact as well as approximate, for calculating flow-fields under the most diverse conditions: with and without heat transfer from the object, with suction or blowing from the solid surface, with variable fluid properties, and so on. This truly great advance in the science of fluid mechanics has come about with the development and application of boundary-layer theory.

Boundary-layer theory is essentially a perturbation technique which, starting from the steady-state limiting solution of the Navier–Stokes equations for vanishing viscosity, enables the construction of solutions for small but finite viscosity.§ Clearly then, knowledge of the correct limiting solution is an essential prerequisite for the success of such an approach. Undoubtedly, in the case of flow past slender objects, the limiting solution is the corresponding continuous potential-flow solution, and no ambiguity seems to exist concerning the general nature of the steady flow at high Reynolds numbers. It is well known, however,

* Present address: Fairchild Semiconductor Research Laboratories, Palo Alto, California.

† Present address: General Electric Company Space Sciences Laboratory, King of Prussia, Pennsylvania.

‡ Present address: Stanford University, Stanford, California.

§ In this context, the word 'viscosity' is used in a dimensionless sense, i.e. the reciprocal of the Reynolds number.

that for flow past bluff bodies, where separation of the flow from the solid surface takes place, the continuous potential flow solution yields a pressure distribution that is so grossly inaccurate that it cannot be used to predict either the drag or, via a standard boundary-layer type analysis, the rates of transport of vorticity, heat and mass from the surface to the streaming fluid. It appears therefore that the continuous potential flow solution is not the correct limiting solution for flows where separation occurs, and that, before such flows could be analysed rigorously, the correct limiting or asymptotic solution for steady separated flows would have to be found (Goldstein 1960).

How to obtain this limiting solution is an old question which still remains substantially unanswered. From a theoretical stand-point one may of course assume that, just as for the streaming flow past slender objects, the thickness of the regions where the effects of viscosity cannot be neglected vanishes with vanishing viscosity, such regions becoming everywhere infinitesimally thin shear layers in the limit. Yet, even if this simplified point of view is adopted, the problem still remains unsolved; for, when separation takes place, these shear layers leave the surface of the solid body and their position becomes unknown. Nor can experimental observations be of much help. As a rule, separated flows become unstable at relatively low Reynolds numbers and few conclusions, if any, can be drawn from such unsteady flows regarding the asymptotic nature of the steady flow at large Reynolds numbers. A third approach, involving the numerical solution of the full Navier–Stokes equations, has also been tried, but here the calculational difficulties mount greatly as the Reynolds number is increased since a very small mesh size is required at large Reynolds numbers for any proper description of the flow field. Consequently, numerical solutions have been performed only up to a Reynolds number of 40 (Thom 1933; Kawaguti 1953*b*; Apelt 1961), which is not large enough to reveal the asymptotic character of the steady flow.

Under such conditions, therefore, it has been found necessary to introduce into the analysis of this problem a number of postulates which could not be substantiated by experimental observations. Perhaps the most important assumption that has customarily been made is that the limiting solution of the Navier–Stokes equations for the case of vanishing viscosity will be a solution of the limit of the equations, namely the Euler equations. Even so, an important difficulty immediately arises for separated flows. The Euler equations possess not one, but an infinite number of solutions (Landau & Lifschitz 1959) and it is impossible to tell *a priori* which one of these, if any, represents the correct limit of the steady flow.

It is convenient now to group the proposed solutions, all of which satisfy the Euler equations, into two broad categories. The first contains the familiar Helmholtz–Kirchhoff free-streamline model in which the wake, enclosed by two free-streamlines, is assumed to consist of a completely stagnant fluid at the same pressure as that of the undisturbed stream. As a result, the width of the wake increases parabolically with distance from the body. The Kirchhoff-flow was proposed as the limiting solution by Squire (1934), Imai (1953) and Kawaguti (1953*a*).

In the other group are solutions having finite wakes or no wake at all. Included are the well-known continuous potential flow model for flow around a circular cylinder (Milne-Thomson 1960), Föppl's vortex model (1913), developed by Shair (1963), which gives a streamline structure rather similar to the one observed in steady flow at moderate Reynolds numbers, and Batchelor's proposal (1956) consisting of a closed wake of finite length within which the vorticity has a constant, non-zero value. All solutions in this group yield a zero pressure drag for the object. This, of course, is contrary to experience with real flows; but, as Batchelor has rightly pointed out, our experience with large Reynolds number motion is limited to unsteady flows and is therefore inapplicable to the hypothetical case of the asymptotic steady flow.

In addition to these solutions of the Euler equations, a number of inviscid flow configurations have been proposed for the more practical purpose of approximating real high Reynolds number flows past bluff bodies. Of these, Roshko's model (Roshko 1954, 1955; Woods 1955; Wu 1956, 1962) deserves special mention. In a sense, it is a modification of the Kirchhoff-flow in that it allows for an arbitrary low wake pressure which can then be adjusted to agree with the experimentally observed value. The Roshko model yields the pressure distribution around a number of objects in good agreement with the experimental results if the wake pressure is properly chosen. In spite of its usefulness, however, this model suffers from the fact that it requires the use of an artifice, the purpose of which is to force a complete pressure recovery in the wake of the body. Also included in this category are Riabouchinsky's plate model (1920) and Gilbarg & Serrin's re-entrant jet model (1950), both of which, however, contain fictitious mathematical devices that render them physically unrealistic.

From what has been said so far, it is clear that our present knowledge concerning the nature of steady separated flows at high Reynolds numbers is quite limited, and that a much better insight into the basic mechanisms and phenomena involved could be obtained from a detailed experimental study of flows with steady wakes, such as the streaming motion past a circular cylinder, rather than from a continued synthesis of new mathematical models. To be sure, the steady separated flow past a circular cylinder has been studied before experimentally (Thom 1933; Homann 1936*a* and Taneda 1956), but, because of the onset of instability at a Reynolds number as low as 40,* these studies yield little information about the asymptotic nature of the steady flow. Recent findings, however, regarding the stabilizing influence of the confining walls of the experimental equipment (Shair, Grove, Petersen & Acrivos 1963) and of a downstream splitter plate (described in the Appendix) made it possible for us to extend these experimental studies up to a Reynolds number of about 300, which it was hoped would be large enough to provide us not only with a better understanding of the limiting character of the steady separated flow, but also with a firmer basis either for selecting one of the already existing inviscid models or for developing an improved theoretical solution to this general problem.

In what follows, we shall present the principal features of an experimental

* The Reynolds number is $R = Ud/\nu$, where U is the velocity of the undisturbed stream, d is the cylinder diameter and ν is the kinematic viscosity.

investigation of the steady separated flow past a circular cylinder in the Reynolds number range of about 30 to 300. Of particular interest are the pressure distribution around the cylinder, the structure of the steady wake, as well as the magnitude of the backflow velocity within the wake, all of which were determined with the aid of an oil tunnel and some rather novel experimental techniques. Since the chief objective of this study was to establish experimentally the asymptotic nature of the steady flow, considerable emphasis was placed upon observing the variation of the flow characteristics with increasing Reynolds

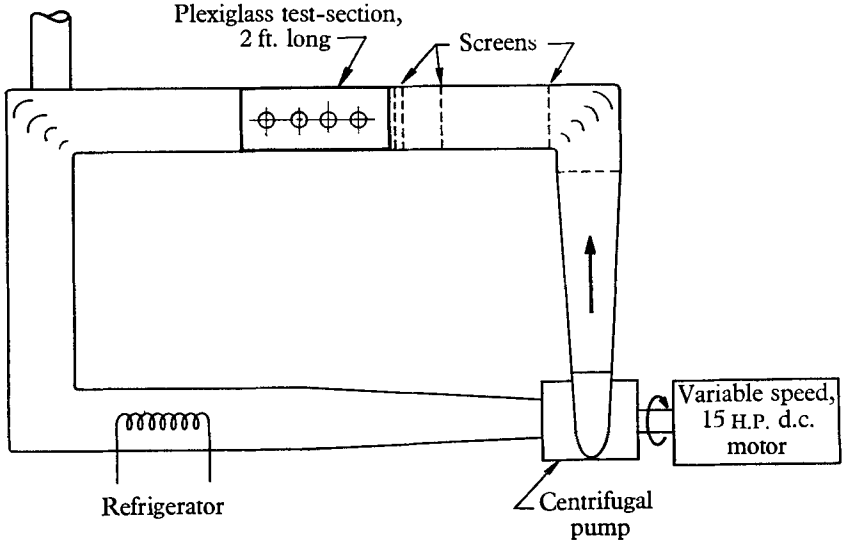

FIGURE 1. Schematic illustration of the oil tunnel (approximately to scale).

number. Yet, particular attention was also paid to the possible effect of the presence of the walls and the splitter plate on the experimental results, in order to ascertain with some confidence whether or not these results would still be valid in the ideal case of a truly two-dimensional, infinite flow-field without a splitter plate. All these experiments were performed in a tunnel (shown schematically in figure 1 and described in detail by Shah 1961; Shah, Petersen & Acrivos 1962; and by Shair 1963) in which a Newtonian lubricating oil with a viscosity of about 1 P was recirculated past a horizontal circular cylinder placed in the centre of the test section with its axis normal to the direction of the main flow.

2. Pressure measurements

(*a*) *Experimental technique*

Pressures on the cylinder surface were measured by a simple manometer technique. A small hole was drilled into the cylinder, exactly half-way between its two ends, and then connected to a vertical glass tube where the oil level could be read by means of a cathetometer with an accuracy of about $\pm 0{\cdot}005$ cm. The cylinder could be rotated about its axis and the position of the hole relative to

the front stagnation point could be established to within $\pm 1°$ by means of a protractor scale. Three such pressure cylinders were used, $\frac{1}{2}$, 1 and $1\frac{7}{8}$ in. in diameter, respectively.

Before the pressure measurements could be interpreted properly, it was found necessary to determine first of all the correct static pressure and the correct characteristic velocity for the flow. Clearly, in the case of a cylinder immersed in an unbounded uniform stream there is no ambiguity in the definition of these two quantities: they are the constant pressure and velocity of the stream far away from the cylinder. For low Reynolds number flow in a tunnel or a channel, however, the fluid velocity and pressure vary significantly along the axis of the test section, even in the absence of the cylinder, due to the boundary layer built up along the walls of the equipment.

In order to overcome this difficulty, the following compromise was adopted. The static pressure was taken to be the pressure measured by means of a manometer fitted to a tap in the bottom of the test section directly below the centre of the cylinder, and the characteristic velocity for a given experiment was chosen to be the velocity which would exist at the location of the centre of the cylinder, under flow conditions identical with those of the experiment, but in the absence of the cylinder. These choices would yield the correct static pressure and characteristic velocity in the limit as the diameter $d \to 0$. How closely they approximated the correct values for a finite value of d could be decided only by experiment.

The actual measurement of the static pressure, as defined above, was quite straightforward. The oil level in the static manometer was measured with the cathetometer, and, since the quantity of interest was always the difference between the cylinder and the static pressure, any capillary effects in the manometer tubes cancelled each other.

The velocity of the oil at various points within the test section was measured in the absence of the cylinder using an air-bubble tracer technique. A correlation was developed which could predict, with a maximum error of about $\pm 5\%$, the velocity at any point along the centre-line of the test section as a function of the viscosity of the oil and the pump speed. Further details, as well as certain interesting observations concerning the velocity profiles and the pressure drop in the tunnel test section (Grove 1963), will not be reported here since they are incidental to the principal contents of this paper.

In what follows we shall make frequent use of the pressure coefficient (hereafter simply referred to as the pressure) at any angle θ from the front stagnation point. It is defined as

$$\hat{p}_\theta = (p_\theta - p_{\text{stat.}})/\tfrac{1}{2}\rho U^2,$$

where p_θ is the actual cylinder pressure, ρ is the fluid density and $p_{\text{stat.}}$ and U are, respectively, the static pressure and the characteristic velocity.

(*b*) *The front stagnation pressure*

We shall next derive a theoretical expression for the front stagnation pressure, $\hat{p}_0$. Along the stagnation streamline $y = 0$, the x component of the Navier–Stokes equations is

$$u\frac{\partial u}{\partial x} = -\frac{1}{\rho}\frac{\partial p}{\partial x} + \nu\left[\frac{\partial^2 u}{\partial x^2} + \frac{\partial^2 u}{\partial y^2}\right]. \tag{1}$$

This can be integrated immediately from the front stagnation point, $x = 0$, to minus infinity upstream of the cylinder to yield

$$\hat{p}_0 = 1 + \frac{\nu}{\frac{1}{2}U^2}\int_{-\infty}^{0}\left[\frac{\partial^2 u}{\partial x^2} + \frac{\partial^2 u}{\partial y^2}\right]dx, \tag{2}$$

which, for a high Reynolds number analysis, can be rearranged into

$$\hat{p}_0 = 1 + \frac{\nu}{\frac{1}{2}U^2}\left\{\int_{-\delta}^{0}\left[\frac{\partial^2 u}{\partial x^2} + \frac{\partial^2 u}{\partial y^2}\right]dx + \int_{-\infty}^{-\delta}\left[\frac{\partial^2 u}{\partial x^2} + \frac{\partial^2 u}{\partial y^2}\right]dx\right\}, \tag{3}$$

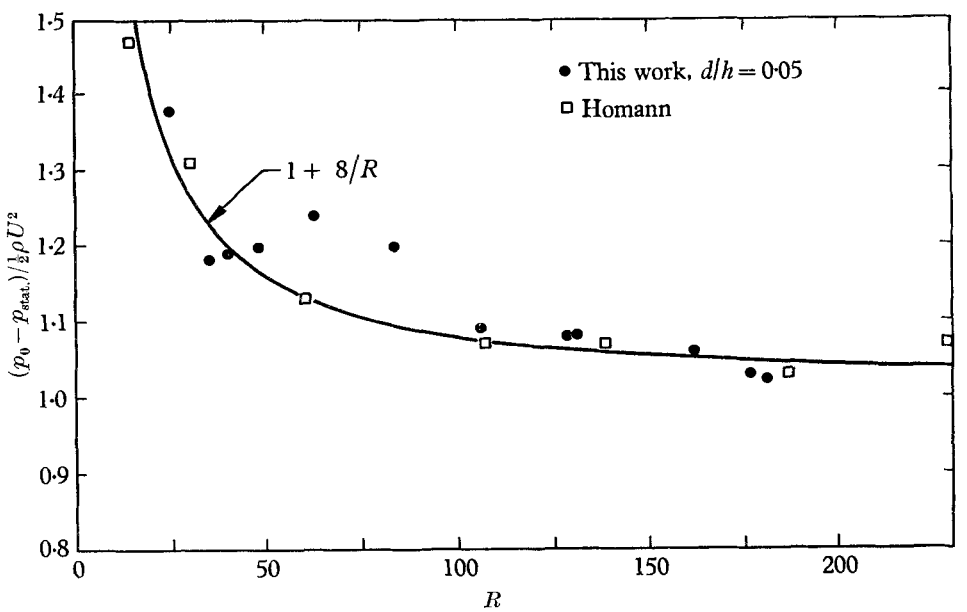

FIGURE 2. The effect of Reynolds number on the front stagnation pressure.

where δ is the boundary-layer thickness. The second integral vanishes because of the irrotationality of the outer flow while in the first integral the usual boundary-layer approximation $\partial^2 u/\partial x^2 \gg \partial^2 u/\partial y^2$ can be introduced. Hence, since

$$\frac{\partial u}{\partial x} = -\frac{\partial v}{\partial y} = 0 \quad \text{at} \quad x = 0,$$

$$\hat{p}_0 = 1 - \frac{\nu}{\frac{1}{2}U^2}\frac{\partial u}{\partial x}\bigg|_{\substack{x=\delta,\\ y=0}} = 1 + \frac{A}{R} + \ldots, \tag{4}$$

where the numerical value of A follows directly from the outer flow solution. Thus, if for example the continuous potential flow solution is selected (this solution holds quite well near the front stagnation point), $A = 8$, and therefore

$$\hat{p}_0 = 1 + (8/R) + \ldots. \tag{5}\dagger$$

† Homann (1936*b*) arrived at this result through a somewhat different reasoning.

Front stagnation pressures, which were measured with the $\frac{1}{2}$ in. diameter cylinder placed into the second porthole of the test-section, are shown in figure 2 (for this cylinder the diameter to tunnel width ratio d/h was 0·05, and the flow could be stabilized up to a Reynolds number of 180 using a splitter plate). Also shown are Homann's (1936*a*) measurements (including those with unsteady wakes), and a curve based on equation (5). Since the expected accuracy in U^2 is only about $\pm 10\%$, the adopted technique appears to be satisfactory.

It should be noted, incidentally, that the presence of a splitter plate behind the cylinder was found to have no effect on the front stagnation pressure.

(c) *Pressure distribution around the cylinder*

The pressure distribution around the $\frac{1}{2}$ in. cylinder at $R = 40$, both with and without the splitter plate, is shown in figure 3 together with similar measurements by Thom (1933) and Homann (1936*a*). The agreement is good in spite of a slight

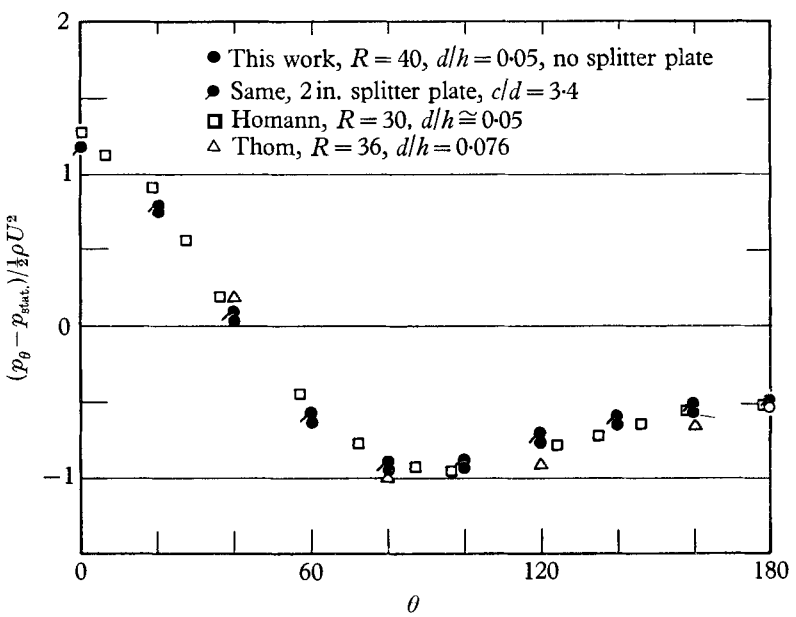

FIGURE 3. The pressure distribution around the cylinder: comparison with previous experiments; the effect of the splitter plate.

difference in the Reynolds numbers. Clearly, the presence of the splitter plate had only a very small effect on the pressure profile. (The parameter c denotes the distance between the centre of the cylinder and the nearer (front) edge of the splitter plate. Thus, when $c = \frac{1}{2}d$, the splitter plate touches the cylinder.) Pressure distributions at three different Reynolds numbers but under otherwise identical conditions are presented in figure 4. From these, the appropriate pressure or form drag coefficients

$$C_{D,p} \equiv \int_0^\pi \hat{p} \cos\theta \, d\theta \tag{6}$$

were calculated, and are shown in figure 5 together with Thom's (1933) and Homann's (1936*a*) earlier results. Roshko's data (1955), which were obtained at much higher Reynolds numbers than encountered in the present work, are also shown in this figure even though it is not clear whether the use of the long

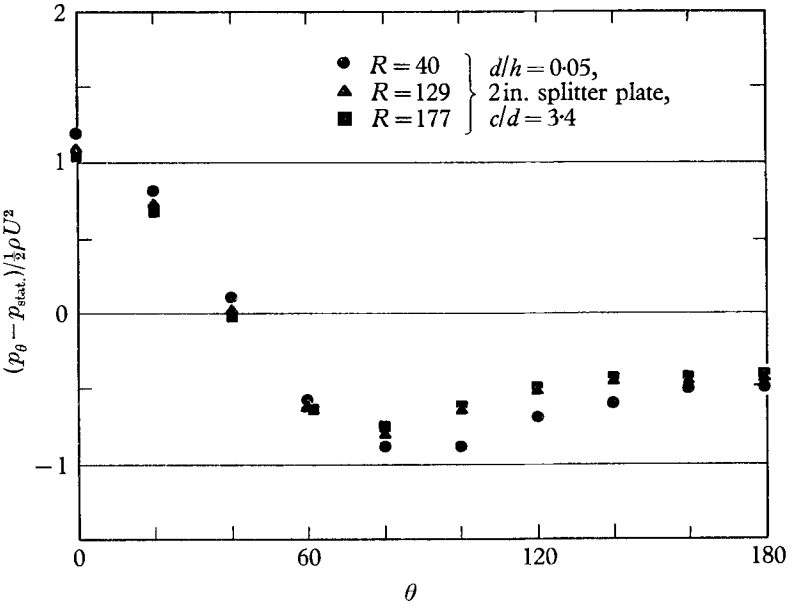

FIGURE 4. The effect of Reynolds number on the pressure distribution around the cylinder.

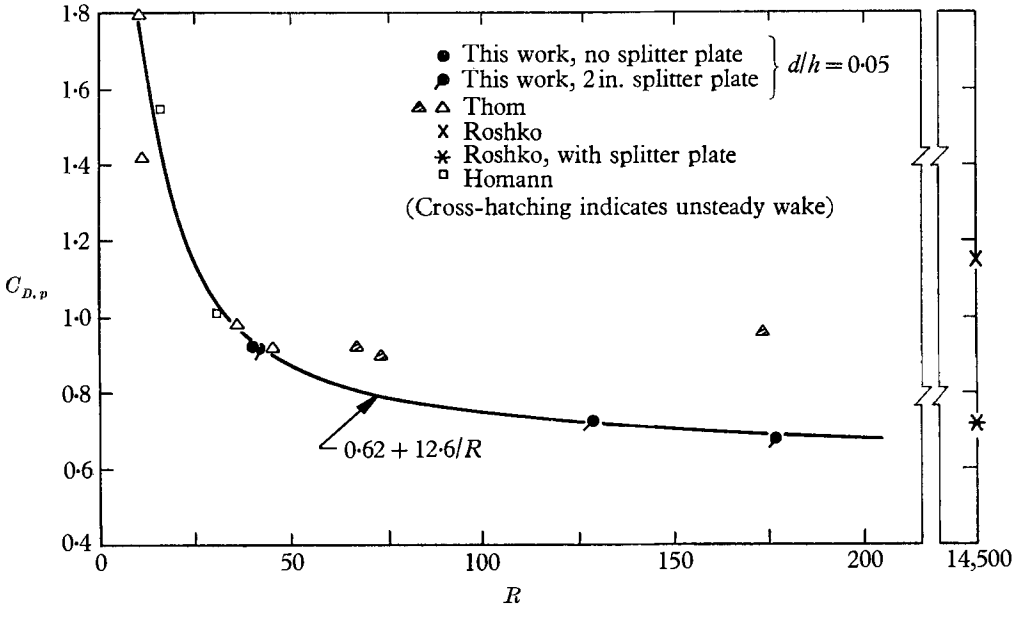

FIGURE 5. The effect of Reynolds number on the pressure drag coefficient.

splitter plate in his experiments did in fact stabilize the wake (Roshko only reports prevention of vortex shedding).

It is evident from figure 5 that the empirical expression

$$C_{D,p} = 0{\cdot}62 + 12{\cdot}6/R \tag{7}$$

is in excellent agreement with the points pertaining to steady wakes, and that, at higher Reynolds numbers, there is an increasing deviation between the pressure drag coefficients for flows with steady and unsteady wakes.

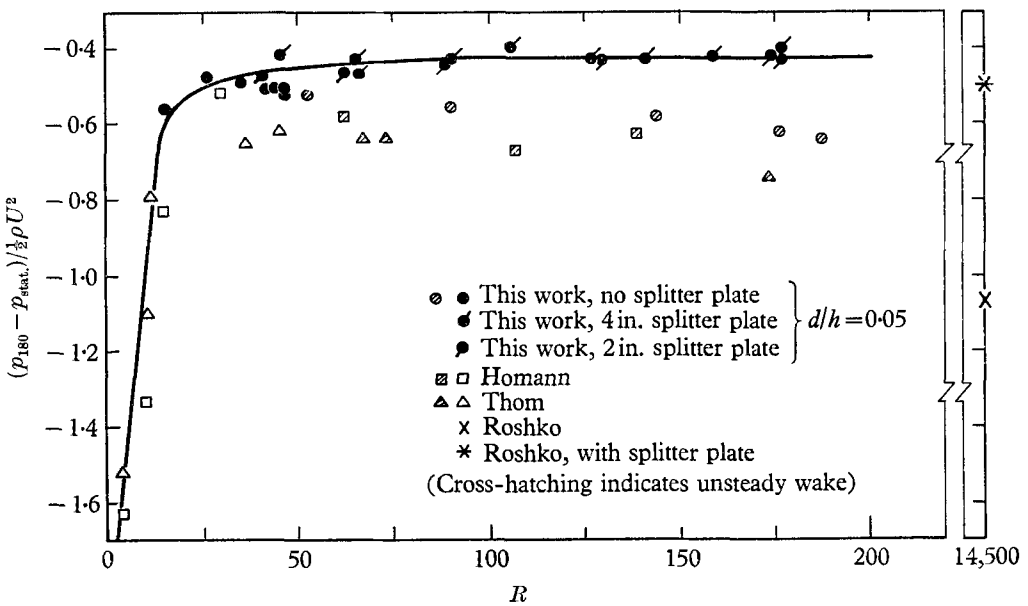

FIGURE 6. The effect of Reynolds number on the rear stagnation pressure.

The pressure at the rear stagnation point, representative of the wake pressure, was recognized as a particularly important parameter and, for this reason, it was measured under a wide variety of conditions with the wake both steady and unsteady. The results of these measurements are shown in figure 6.

Two important conclusions can immediately be drawn from this figure regarding steady wakes. First, that the rear pressure quickly reaches a limit of approximately $-0{\cdot}45$ as the Reynolds number is increased; and second, that this limit is attained, for all practical purposes, at a Reynolds number as low as 25.

(*d*) *Wall effect*

The pressure distribution was also measured using the 1 in. and $1\frac{7}{8}$ in. diameter cylinders in order to study the effect of the proximity of the confining walls. The results, together with the data obtained with the $\frac{1}{2}$ in. cylinder, are shown in figure 7. It can be seen that the general shape of the pressure profile is not changed and that the magnitude of the wall effect is not excessively large.

One can gain some insight into the reasons behind the wall effect by considering figure 8, plate 1. This photograph of the test section was taken with the

tunnel almost full and with a 2 in. diameter cylinder in the second porthole. The shape of the free surface, which approximately corresponds to the 'static' pressure variation in a completely full test section, indicates the large effect which the presence of the cylinder exerts on the flow. Clearly, the pressure measured directly below the cylinder is no longer representative of the 'effective' static pressure under such conditions. Indeed, if the variation of the background pressure is taken into account in an approximate manner, the difference between the pressure distributions around the $\frac{1}{2}$ in. and the $1\frac{7}{8}$ in. cylinders is about halved.

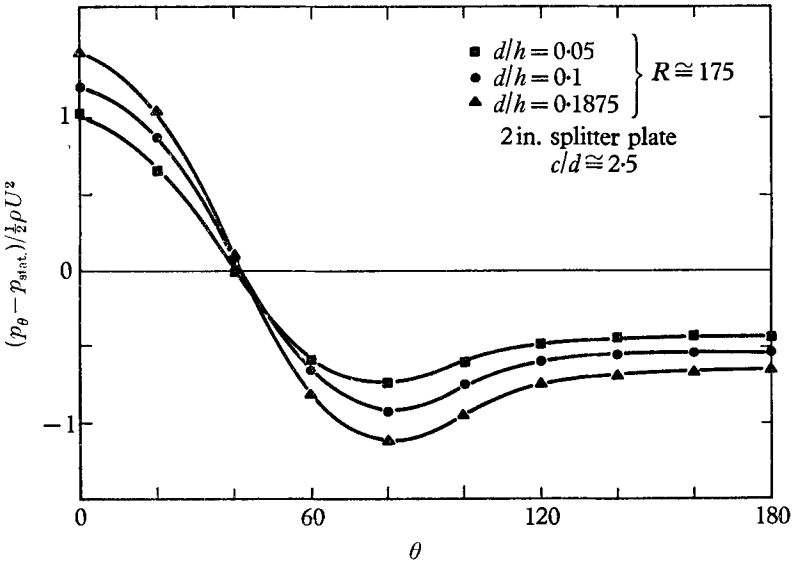

FIGURE 7. The effect of confining walls on the pressure distribution.

The pressure drag coefficient was increased by the presence of the walls. For example, at a Reynolds number of about 180, the pressure drag coefficient was found to be 0·68 for $d/h = 0{\cdot}05$, 0·91 for $d/h = 0{\cdot}1$ and 1·06 for $d/h = 0{\cdot}1875$. However, in spite of this seemingly large dependence of the drag on the d/h ratio, there are good reasons for believing that the limiting form of the pressure profiles for $d/h \to 0$ has already been reached where $d/h = 0{\cdot}05$. First of all, there is the satisfactory agreement, shown in figure 2, between the experimentally determined stagnation pressures and equation (5), which was derived on theoretical grounds. This agreement is still retained, incidentally, even if the numerical value of the constant A in equation (4) is calculated from the actual pressure distribution at $R = 177$ rather than from the continuous potential flow solution (its value is changed from 8 to 7·76). Also, there is agreement with Tritton's (1959) total drag measurements for which the d/h ratio was practically zero. At $R = 40$, probably the highest value of the Reynolds number at which the wake was steady, Tritton reports a total drag coefficient of about 1·5. On the other hand, for $d/h = 0{\cdot}05$, our experiments yield a pressure drag coefficient of 0·94, to which must be added the friction drag coefficient. The latter can be

estimated by means of a standard laminar boundary-layer analysis using the measured pressure profile. The skin friction coefficient is thus found to be approximately equal to 0·46, which, when added to 0·94, results in a total drag coefficient of 1·4 in essential agreement with Tritton's value.

3. Development of the steady wake

(*a*) *The wake-bubble boundary*

In steady separated flow there is a closed region of recirculating, vortex type motion behind the cylinder which, due to its closed nature, appears very much like a bubble. Some of the features of such a typical wake-bubble are shown in figure 9. Of these, the streamline which constitutes the boundary of the wake-bubble, extending from the separation point to the wake stagnation point, is of particular importance as it separates two distinct flow regions: the inner, vortex type flow, and the outer flow past the cylinder and the wake-bubble.

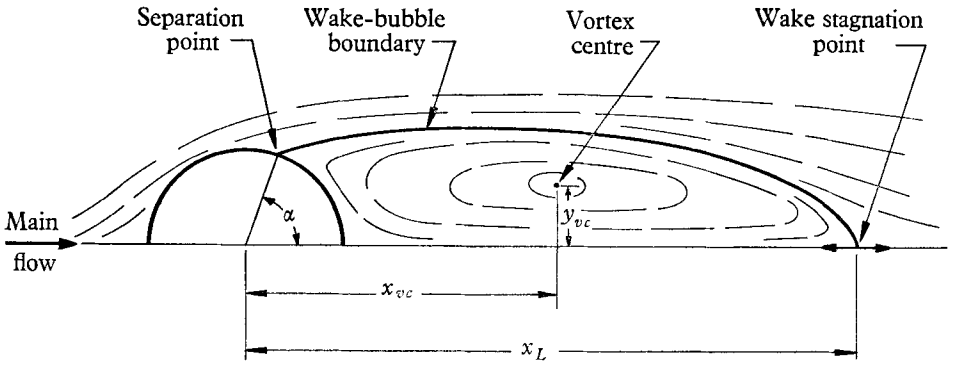

FIGURE 9. The steady separated flow past a circular cylinder.

Under ordinary circumstances the wake-bubble boundary is invisible. Thom distinguished it by an ink injection technique and Homann by the addition of tracer particles to the fluid. An alternative method was discovered by Shair (1963), who noticed that when the cylinder is heated the temperature of the fluid along the wake-bubble boundary is higher than elsewhere. This sharp local temperature variation is accompanied by a jump in refractive index and, as a result, the wake-bubble boundary becomes visible and can even be photographed. That this visual effect indeed takes place at the wake-bubble boundary as defined above was verified by the observation of the motion of tiny air-bubble tracers in the flow field around the cylinder.

The reason for the existence of higher fluid temperature along the wake-bubble boundary is clear in view of Shair's heat transfer experiments which showed that the maximum cylinder temperature occurred at the separation point. Hence, the temperature of the fluid along the streamline coming from the separation point (the wake-bubble boundary) will also be higher than elsewhere.

At some distance downstream from the cylinder the higher local temperature of the wake-bubble was dissipated and the visual effect diminished; for this

reason, only part of the wake-bubble boundary could be observed. This part was accentuated by placing a vertical grid between the test section and the light source. Typical photographs taken with this arrangement at different Reynolds numbers, using a 2 in. diameter heated cylinder, are presented in figures 10 to 12, plate 2. (Flow is from right to left. The black circle is the image of the cylinder; the other circle downstream of it is the neighbouring porthole. The splitter plate appears as a thin line in the vicinity of the downstream porthole.) In obtaining these photographs, the camera was focused at the outline of the wake-bubble midway between the two faces of the cylinder. For this reason the nearer face of the cylinder (black circle) appears on the photographs somewhat larger than in reality. In the composite diagram, figure 13, which was prepared from the photographs by tracing out the visible part of the wake-bubble boundary, a correction was made for this perspective effect.

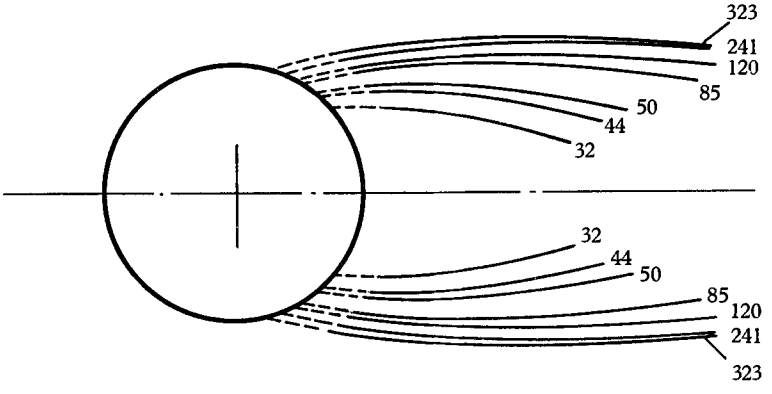

FIGURE 13. Development of the wake-bubble boundary with Reynolds number.

The perspective effect also made it difficult to obtain the angle of separation, α, directly from the photographs and a simple visual procedure was therefore adopted for this purpose. A circular paper disk was fitted to the face of the cylinder and on this disk the positions of both separation points were marked. Great care was taken to make the markings while sighting along that generator of the cylinder where separation took place. The paper disk was then removed and the angle between each of the separation points and a horizontal line was measured.† This visual method is believed to be accurate within $\pm 3°$. As expected, the individual separation points were affected by the heating of the cylinder since, especially at lower Reynolds numbers, a slight upward tilting of the wake-bubble was observed which was undoubtedly due to natural convection. This, however, did not appear to influence the average value of the two

† It should be carefully noted, however, that since the outline of the wake-bubble boundary appeared diffuse in the vicinity of the cylinder, the so-called separation angle, α, had to be determined by extrapolating the visible part of this boundary up to the cylinder. It is believed, therefore, that the values of α reported here may not correspond exactly to the true separation point, i.e. the point at which the outer flow detaches itself from the surface of the cylinder.

separation points, nor, incidentally, did it affect the stability of the steady wake. In some of the experiments, the separation points were also located by observing the motion of tiny air-bubble tracers in the vicinity of the unheated cylinder. Although this method was less reproducible than the one described above, it served as an independent check on the reliability of the heating method.

In view of the above observations, the composite diagram of the wake-bubble boundary, figure 13, contains a correction for the slight tilting of the wake, and the separation angles shown in figure 14 are the averages of the upper and the lower values. Also included in figure 14 are the control data with the air-bubble tracers and a number of results from other investigations.†

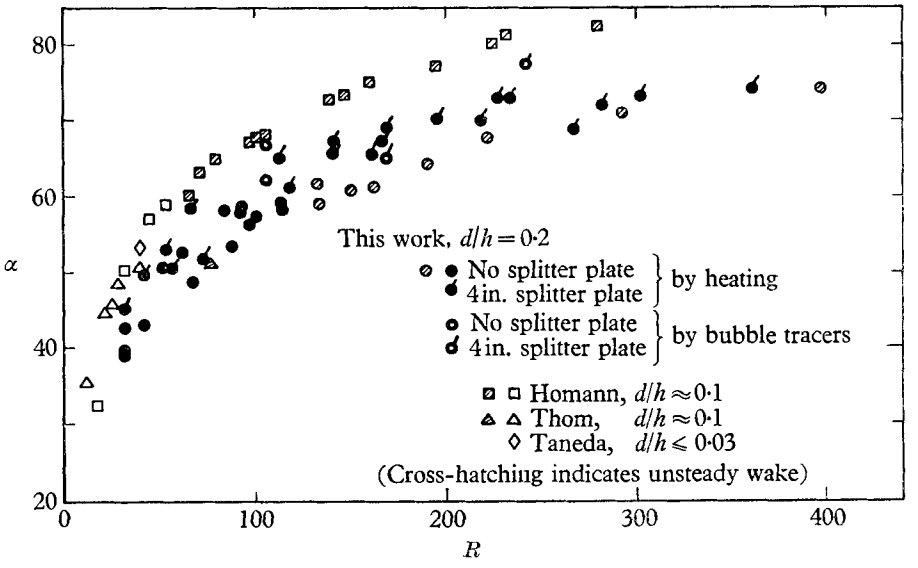

FIGURE 14. The effect of Reynolds number on the angle of separation.

The present data appear to be about 5–10° below Homann's and Thom's. This deviation may be due to the different d/h ratios encountered in these cases. Whether this is indeed so could not be verified, because, with the experimental equipment used in the present work, meaningful determinations of the separation point could be made only with the 2 in. cylinder. At any rate, the deviations are not excessive. The presence or position of the splitter plate did not have any noticeable effect either on the shape of the wake-bubble or on the angle of separation.

(*b*) *The internal structure of the wake-bubble*

The experimental technique which was used to study the details of the flow within the wake-bubble was essentially visual in nature. The motion of numerous tiny air-bubble tracers around the cylinder was observed and photographed (by

† Homann's (1936*a*) data were read from a small-scale graph; how the data were originally obtained is not described in his paper. Thom's (1933) data were taken directly from his photographs and may well contain a perspective error.

1–2 sec time exposure) with the test-section illuminated from top and bottom by floodlights. The photographs presented in figures 15–17, plates 3–5, illustrate the nature of the flow within the wake-bubble at three different Reynolds numbers. (The white spots were caused by the reflexion of light from screw holes drilled into the wall of the test section.)

In taking these photographs, the camera, which had a depth of field of about $\frac{1}{4}$ in., was focused on the vertical centre-plane of the test-section. For this reason, only air bubbles moving in the vicinity of this centre-plane appear on the photographs; light coming from other air bubbles was diffuse and affected the photographs only by reducing their contrast. Further details of this technique are presented by Shair (1963).

It is evident that the recirculating vortex-type motion, which had been known to characterize the steady wake at relatively low Reynolds numbers, persists as the Reynolds number is increased, provided that the wake remains steady. A similarity between wake-bubbles of different lengths was also observed.

Through the visual observations of the motion of the air-bubble tracers, certain qualitative conclusions could be drawn concerning the magnitude of the velocity of the fluid in and about the wake-bubble. Thus, it was noted that the fluid within the wake-bubble moved considerably slower than in the main stream. Similarly, one could observe the existence of a comparatively slow region just outside the wake-bubble boundary in the neighbourhood of the wake stagnation point, the thickness of which was of the same order of magnitude as the cylinder diameter regardless of the length of the wake-bubble.

The development of the wake-bubble with the Reynolds number was studied more quantitatively by observing the positions of the wake stagnation point and the vortex centre. These are two well-defined points which were easy to locate visually through the motion of the air-bubble tracers. The distance between the wake stagnation point and the cylinder centre, x_L, is a good indication of the length of the wake-bubble (see figure 9). Measurements of x_L using the 2 and 1 in. diameter cylinders are presented in figures 18 and 19 respectively, where a straight-line relationship between x_L and the Reynolds number for the entire range of the experiments is clearly evident. The straight lines drawn through the lower Reynolds number data of figures 18 and 19 are also shown in figure 20 together with the experimental results of Homann (1936*a*) and Taneda (1956). It is apparent that the proximity of the walls tends to shorten the wake-bubble.†

The effect of the presence of a splitter plate within the wake-bubble can also be seen from figures 18 and 19. After the wake stagnation point had reached the nearer (front) edge of the splitter plate, the length of the wake-bubble was

† It is worth while to point out here that the static pressure drop along the length of a wake was quite small in comparison to $\hat{p}_{180}$, the pressure coefficient at the rear stagnation point of the cylinder. For example, even for a value of x_L as large as 4 in. (corresponding to $d = \frac{1}{2}$ in. and $R \sim 180$) the total pressure drop across the length of the wake was less than $0{\cdot}1 \times \frac{1}{2}\rho U^2$ (Grove 1963), whereas $\hat{p}_{180}$ was, under these conditions, equal to $-0{\cdot}45$. Thus, it is safe to conclude that the values for $\hat{p}_{180}$ as measured with the $\frac{1}{2}$ in. cylinder are not indicative of the static pressure drop along the wake, but, rather, are representative of a fundamental parameter of the separated flow.

reduced, but the position of the splitter plate had no noticeable effect on x_L once the splitter plate was entirely within the wake-bubble. It should be pointed out in addition that neither the proximity of the walls nor the presence of the splitter plate appeared to have influenced the nature of the straight-line relationship between wake-bubble length and Reynolds number, and that only the slopes of these lines were affected.

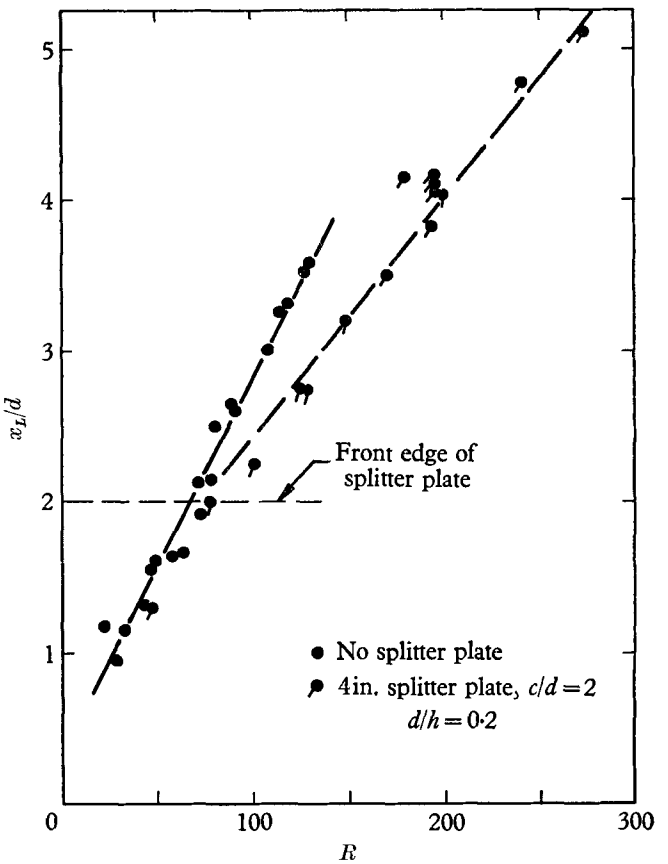

FIGURE 18. The effect of Reynolds number on the length of the wake bubble.

Measurements of the position of the vortex centre (the centre of recirculation within the wake-bubble; see figure 9) using the 2 in. cylinder are shown in figure 21. It is evident from this figure that while the two twin vortex centres move downstream with increasing Reynolds number, their distance from the line of symmetry reaches a limit.

The presence of a splitter plate within the wake-bubble does, of course, interfere with the recirculating motion. For this reason, both the presence and the position of the splitter plate can be expected to influence the location of the vortex centre. Such effects are believed to be responsible for the relatively strong scatter of the data in figure 21, although no systematic influence could be established.

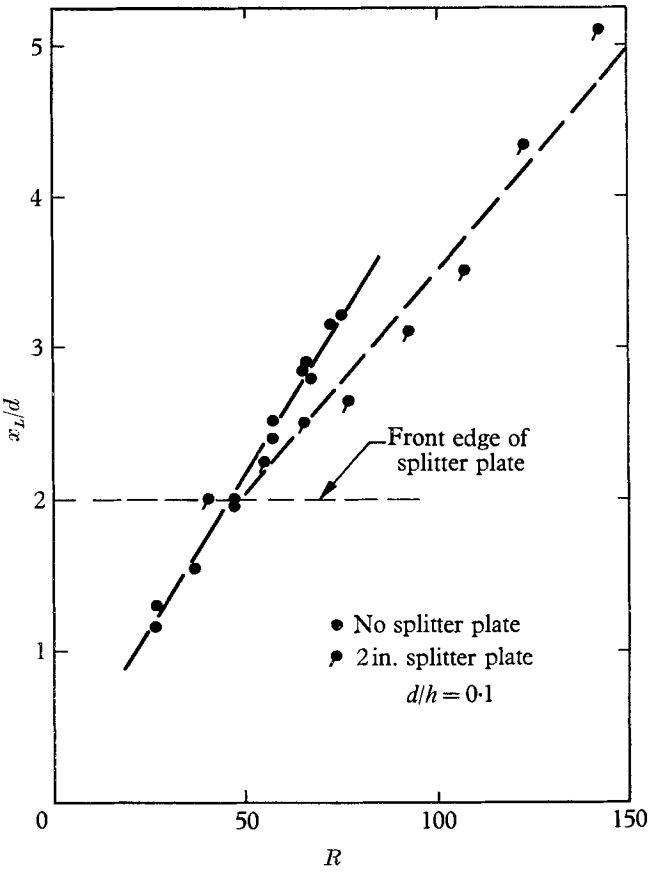

FIGURE 19. The effect of Reynolds number on the length of the wake-bubble.

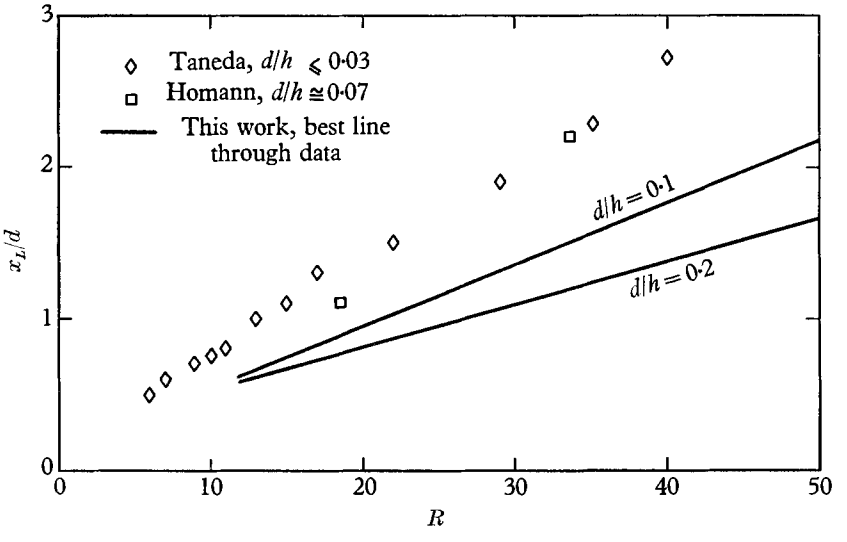

FIGURE 20. The effect of confining walls on the length of the wake-bubble.

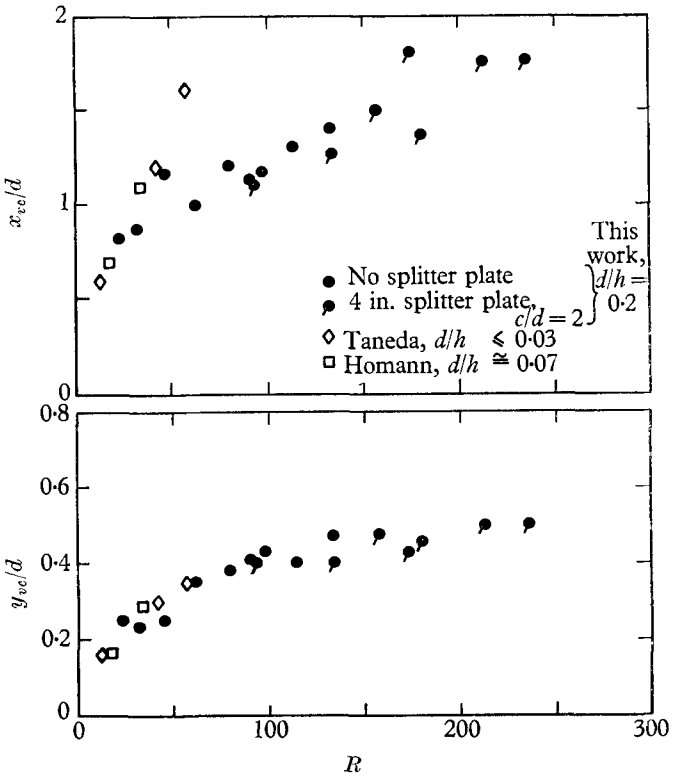

FIGURE 21. The effect of Reynolds number on the position of the vortex centre.

(c) *The velocity along the returning stagnation streamline*

The magnitude of the recirculation velocity within the wake-bubble relative to the velocity of the undisturbed flow is of very great interest, and especially its dependence on the Reynolds number. Yet, because of obvious experimental difficulties, no such measurements appear to have ever been undertaken.

In the present work, the fluid velocity within the wake-bubble was measured along the returning stagnation streamline (the streamline leading from the wake stagnation point to the rear of the cylinder) by using the stroboscopic air-bubble tracer technique reported elsewhere (Grove 1963). The word 'returning' indicates that the direction of the flow here is opposite to that of the undisturbed flow.

Figure 22 shows the variation of the backflow velocity along the returning stagnation streamline with distance from the cylinder. Three sets of such measurements were obtained by using the 2 in. diameter cylinder and air bubbles injected with the hypodermic needle. These data, represented by solid symbols, illustrate the nature of the variation of the velocity along that part of the returning stagnation streamline which is closer to the cylinder. (The heavy dotted line represents the inferred fluid velocity, while the light dotted line indicates the initial acceleration of the air bubbles upon injection into the fluid.) The remaining

set of measurements, represented by the open circles, were obtained with the 1 in. cylinder and with air bubbles freely suspended in the fluid (i.e. not injected with the hypodermic needle). These data illustrate the nature of the variation of the velocity nearer to the wake stagnation point. While the measurements are by no means conclusive, the indication appears to be that the velocity varies

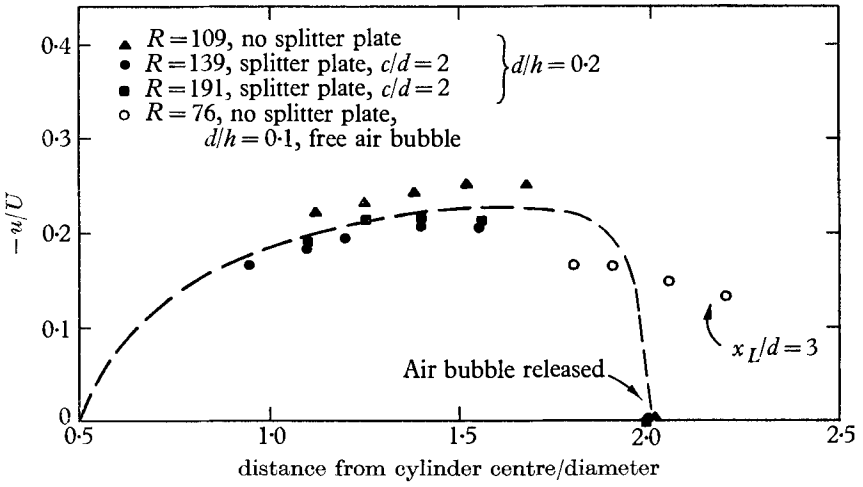

FIGURE 22. The backflow velocity along the returning stagnation streamline.

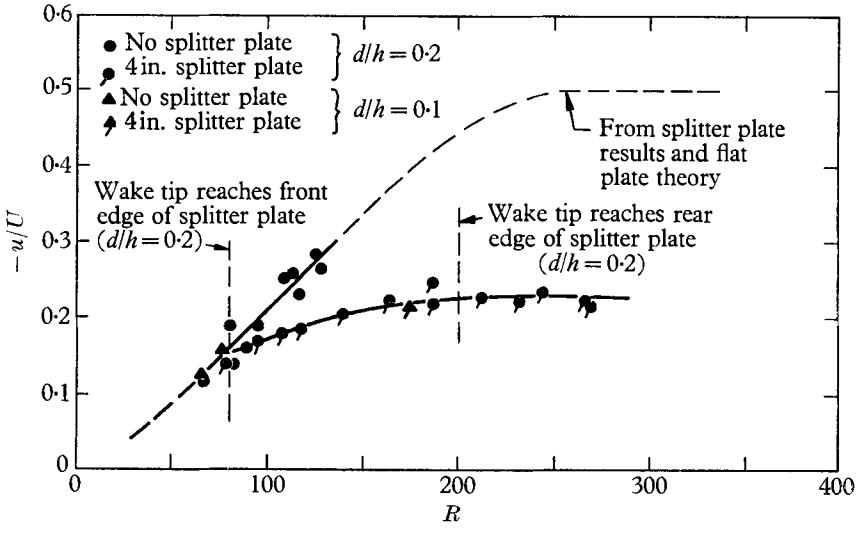

FIGURE 23. The maximum backflow velocity ratio.

evenly along the returning stagnation streamline and that it reaches a maximum value at approximately that point which is closest to the vortex centre.

The maximum backflow velocity, which seemed to be a suitable characteristic of the recirculation rate within the wake-bubble, was studied in further detail using both the 1 and 2 in. diameter cylinders. The results are presented in figure 23, from which it is evident that the splitter plate strongly reduces the

backflow velocity.† As a result of this, the true undisturbed limit of the maximum backflow velocity ratio for large Reynolds numbers could not be established directly. Still, such a limit clearly exists and its magnitude is larger than 0·23 (the limit with the splitter plate present). By correcting for the retarding influence of the splitter plate, on the basis of either Goldstein's theory (1933) for the velocity recovery behind a flat plate placed parallel to a uniform stream or the experimental results presented elsewhere (Grove 1963), this undisturbed limit of the maximum backflow velocity ratio was estimated to be around 0·5.

4. Conclusions

An experimental investigation was carried out for the purpose of studying certain fundamental characteristics of the steady separated flow past a circular cylinder. Particular attention was paid to the variation of these characteristics with increasing Reynolds number, in the hope that the asymptotic nature of such steady flows for the case of very large Reynolds numbers could thereby be inferred. Such an investigation became possible when it was found that the steady separated flow past a cylinder could be artificially stabilized up to a Reynolds number of about 300, without significantly distorting other characistics of the flow, by the presence of a wall effect and by the use of a splitter plate within the wake.

The more significant results of this study are the following: (i) The rear pressure coefficient reaches the value of approximately $-0{\cdot}45$ at $R = 25$ and remains unchanged up to $R = 177$. (ii) The pressure drag coefficient of the cylinder as a function of the Reynolds number is given by

$$C_{D,p} = 0{\cdot}62 + 12{\cdot}6/R \quad \text{for} \quad 10 \leqslant R \leqslant 177.$$

(iii) The character of the wake-bubble behind the circular cylinder remains unchanged as the Reynolds number is increased and the vortex type circulation persists. Also, a similarity between wake-bubbles of different lengths is observed. (iv) The wake-bubble elongates with increasing Reynolds number in such a way that its length is proportional to the Reynolds number for $6 \leqslant R \leqslant 280$. (v) The magnitude of the maximum backflow velocity ratio along the returning stagnation streamline reaches a limit of 0·23 as the Reynolds number is increased with the splitter plate present. If allowance is made for the retarding influence of the splitter plate, the undisturbed ratio is estimated to reach a limit of 0·5.

Thus, a substantial amount of additional information concerning the behaviour of steady separated flows is now available, to enable us to construct a model for the asymptotic flow at large Reynolds numbers with considerably more confidence than would have been justified in the past.

This research project was supported in part by a grant from the Petroleum Research Fund administered by the American Chemical Society. Grateful acknowledgement is made to the donors of said fund.

† As a matter of fact, the maximum return velocity may not necessarily lie along the return streamline when a splitter plate is present.

Appendix

Roshko (1955) reported that the vortex shedding phenomenon could be prevented by placing a thin partition, or splitter plate, along the centreline of the wake downstream of a cylinder. Preliminary experiments by Shair (1963) indicated that it was indeed possible to maintain a completely steady wake behind a circular cylinder at Reynolds numbers considerably above the critical (at which fluctuations of the wake normally set in) by the use of such a splitter plate.

Since it was also found that the effectiveness of the splitter plate in stabilizing the steady wake depended on its location relative to the cylinder as well as on its size, an arrangement was devised which allowed us to use several splitter plates of various widths and also to move the plates back and forth in relation to the cylinder. In this arrangement, the splitter plate is held in a rack which in turn is fitted on to Lucite rails mounted on the inside of the walls of the test section. By turning a pinion penetrating into the test-section one can move the rack and therefore the splitter plate into the most favourable position.

It was, of course, always desirable to use the narrowest splitter plate that would still stabilize the wake in order to minimize any distortions of the flow field due to the introduction of the plate. Hence it was important to find the most effective position for the splitter plate. It appeared that any splitter plate was most effective when its edge nearer to the cylinder was about 2 to 3 diameters downstream from the cylinder. If the Reynolds number was increased to a sufficiently large value, any given splitter plate, regardless of its position, eventually failed to stabilize the wake. However, a wider splitter plate could still be effective. In the experiments presented in this work, two splitter plates were used, 2 and 4 in. wide, respectively.

Figure 24, plate 1, shows the photograph of the tunnel test section with the $\frac{1}{2}$ in. cylinder and the 2 in. splitter plate in position.

REFERENCES

Apelt, C. J. 1961 The steady flow of a viscous fluid past a circular cylinder at Reynolds numbers 40 and 44. *Aero. Res. Council, Lond. R & M* no. 3175.

Batchelor, G. K. 1956 A proposal concerning laminar wakes behind bluff bodies at large Reynolds numbers. *J. Fluid Mech.* **1**, 388.

Föppl, L. 1913 Wirbelbewegung hinter einem Kreiszylinder. *Munich Akad. Wiss., Math.-Physik Classe*, 1.

Gilbarg, D. & Serrin, J. 1950 Free boundaries and jets in the theory of cavitation. *J. Math. Phys.* **29**, 1.

Goldstein, S. 1933 On the two-dimensional steady flow of a viscous fluid behind a solid body. *Proc. Roy. Soc.* A, **142**, 545.

Goldstein, S. 1960 *Lectures on Fluid Mechanics*, Ch. 8. London: Interscience.

Grove, A. S. 1963 *Ph.D. Thesis*, University of California, Berkeley.

Homann, F. 1936*a* Einfluss grösser Zähigkeit bei Strömung um Zylinder. *Forsch. IngWes.* **7**, 1.

Homann, F. 1936*b* Der Einfluss grösser Zähigkeit bei der Strömung um den Zylinder und um die Kugel. *Z. angew. Math. Mech.* **6**, 153. Translation: *Nat. Adv. Comm. Aero., Wash., Tech. Mem.*, no. 1334 (1952).

IMAI, I. 1953 Discontinuous potential flow as the limiting form of the viscous flow for vanishing viscosity. *J. Phys. Soc. Japan*, **8**, 399.

KAWAGUTI, M. 1953*a* Discontinuous flow past a circular cylinder. *J. Phys. Soc. Japan*, **8**, 403.

KAWAGUTI, M. 1953*b* Numerical solution of the Navier–Stokes equations for the flow around a circular cylinder at Reynolds number 40. *J. Phys. Soc. Japan*, **8**, 747.

LANDAU, L. D. & LIFSCHITZ, E. M. 1959 *Fluid Mechanics*, p. 18. London: Pergamon Press.

MILNE-THOMSON, L. M. 1960 *Theoretical Hydrodynamics*, p. 154. London: Macmillan & Co., Ltd.

RIABOUCHINSKY, D. 1920 On the steady flow motions with free surfaces. *Proc. Lond. Math. Soc.* **19**, 206.

ROSHKO, A. 1954 A new hodograph for free-streamline theory. *Nat. Adv. Comm. Aero., Wash., Tech. Note*, no. 3168.

ROSHKO, A. 1955 On the wake and drag of bluff bodies. *J. Aero Sci.* **22**, 124.

SHAH, M. J. 1961 *Ph.D. Thesis*, University of California, Berkeley.

SHAH, M. J., PETERSEN, E. E. & ACRIVOS, A. 1962 Heat transfer from a cylinder to a power law non-Newtonian fluid. *A.I.Ch.E. J.* **8**, 542.

SHAIR, F. H. 1963 *Ph.D. Thesis*, University of California, Berkeley.

SHAIR, F. H., GROVE, A. S., PETERSEN, E. E. & ACRIVOS, A. 1963 The effect of confining walls on the stability of the steady wake behind a circular cylinder. *J. Fluid Mech.* **17**, 546.

SQUIRE, H. B. 1934 On the laminar flow of a viscous fluid with vanishing viscosity. *Phil. Mag.* **17**, 1150.

TANEDA, S. 1956 Experimental investigation of the wakes behind cylinders and plates at low Reynolds numbers. *J. Phys. Soc. Japan*, **11**, 302.

THOM, A. 1933 The flow past circular cylinders at low speeds. *Proc. Roy. Soc.* A, **141**, 651.

TRITTON, D. J. 1959 Experiments on the flow past a circular cylinder at low Reynolds numbers. *J. Fluid Mech.* **6**, 547.

WOODS, L. C. 1955 Two dimensional flow of a compressible fluid past given curved obstacles with infinite wakes. *Proc. Roy. Soc.* A, **227**, 367.

WU, T. Y. 1956 A free streamline theory for two-dimensional fully cavitated hydrofoils. *J. Math. Phys.* **35**, 236.

WU, T. Y. 1962 A wake model for free-streamline flow theory. *J. Fluid Mech.* **13**, 161.

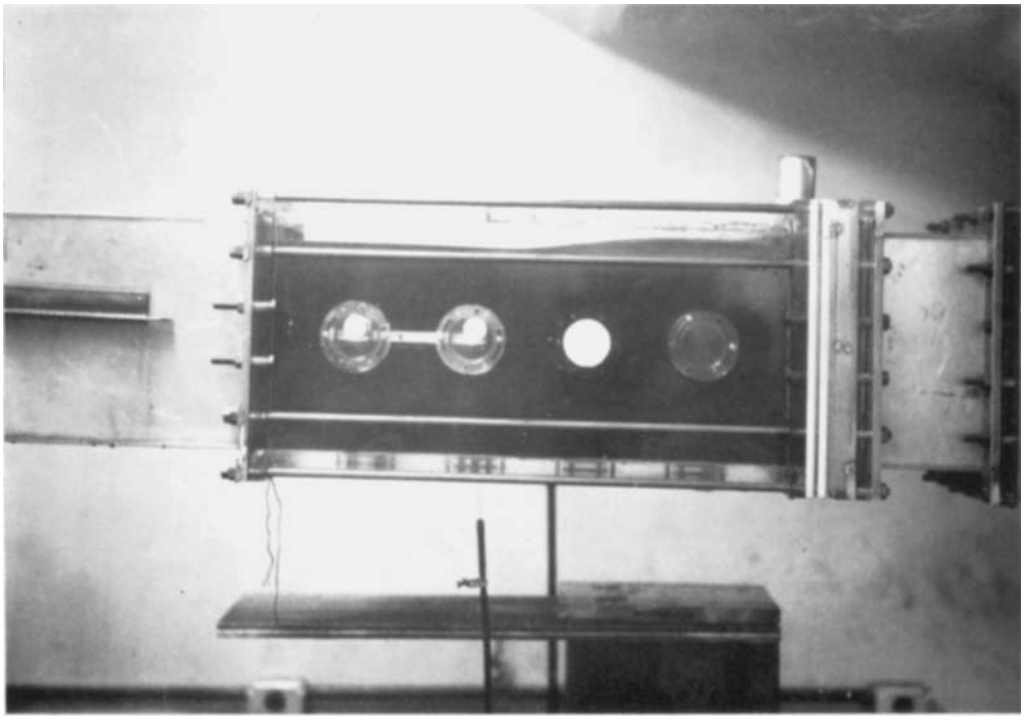

FIGURE 8. The free surface in the test section; tunnel not completely full; 2 in. cylinder in second porthole.

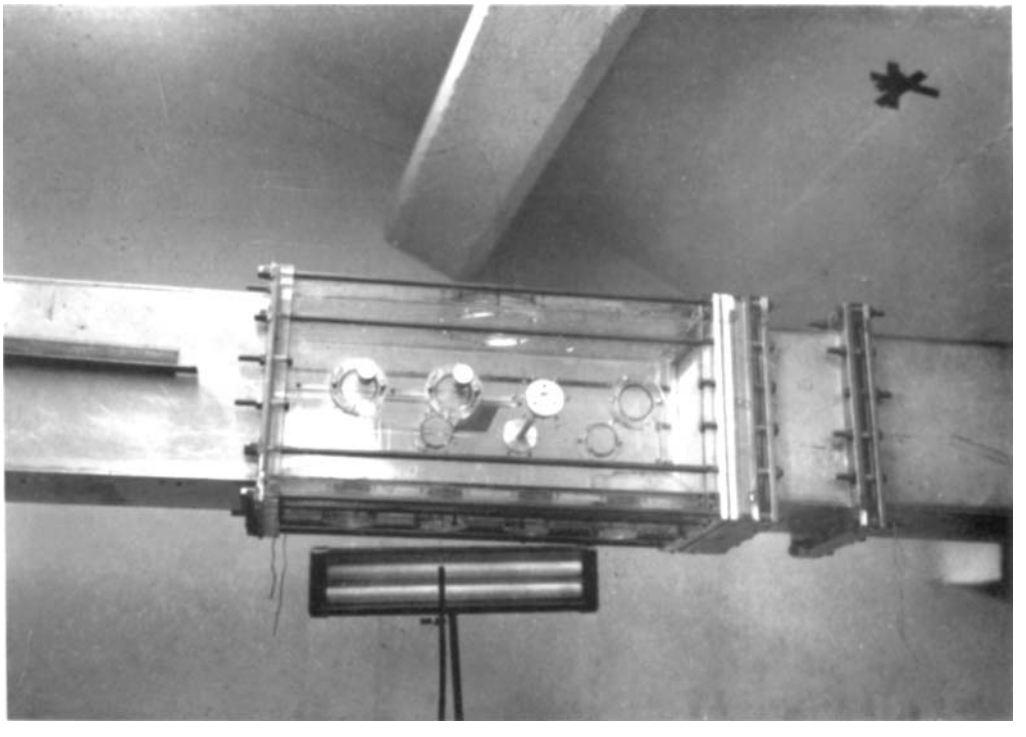

FIGURE 24. The splitter-plate arrangement.

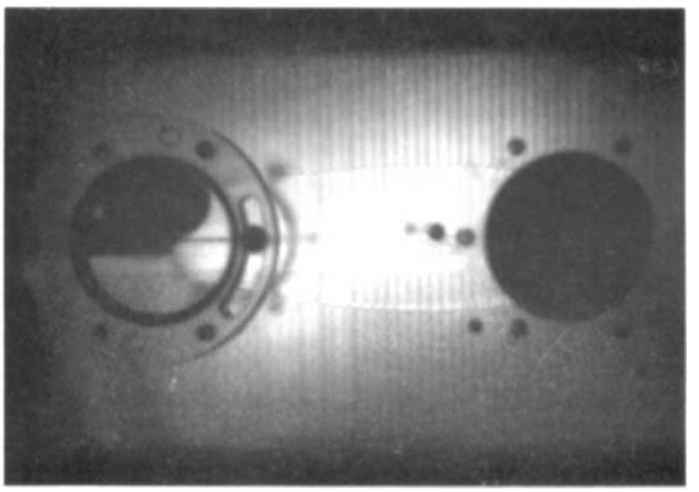

FIGURE 10. $R = 85$.

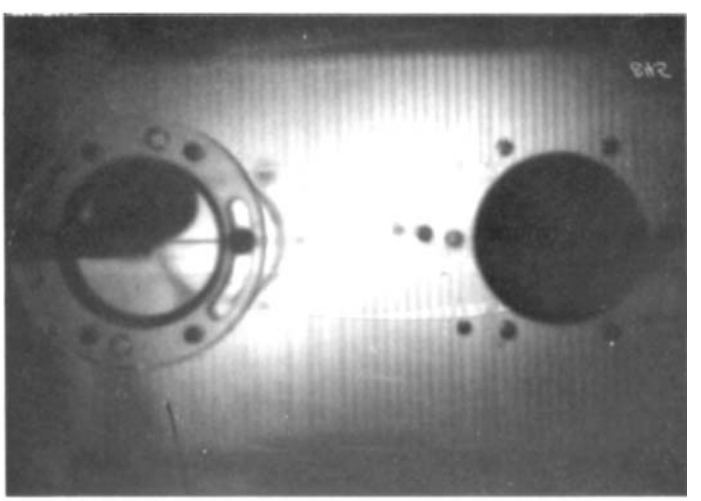

FIGURE 11. $R = 119$.

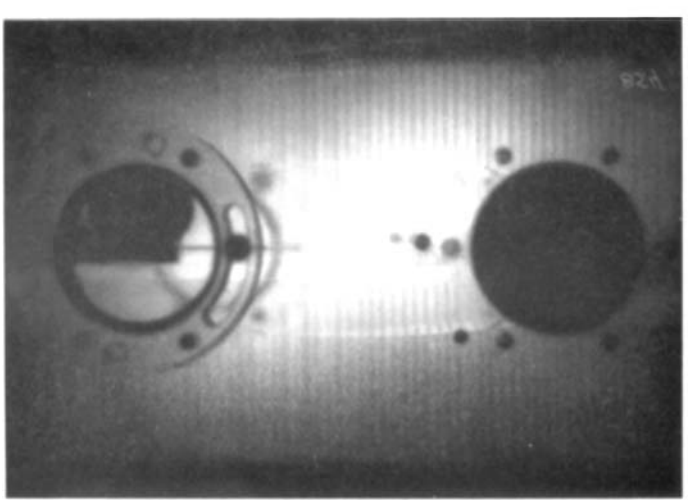

FIGURE 12. $R = 218$.

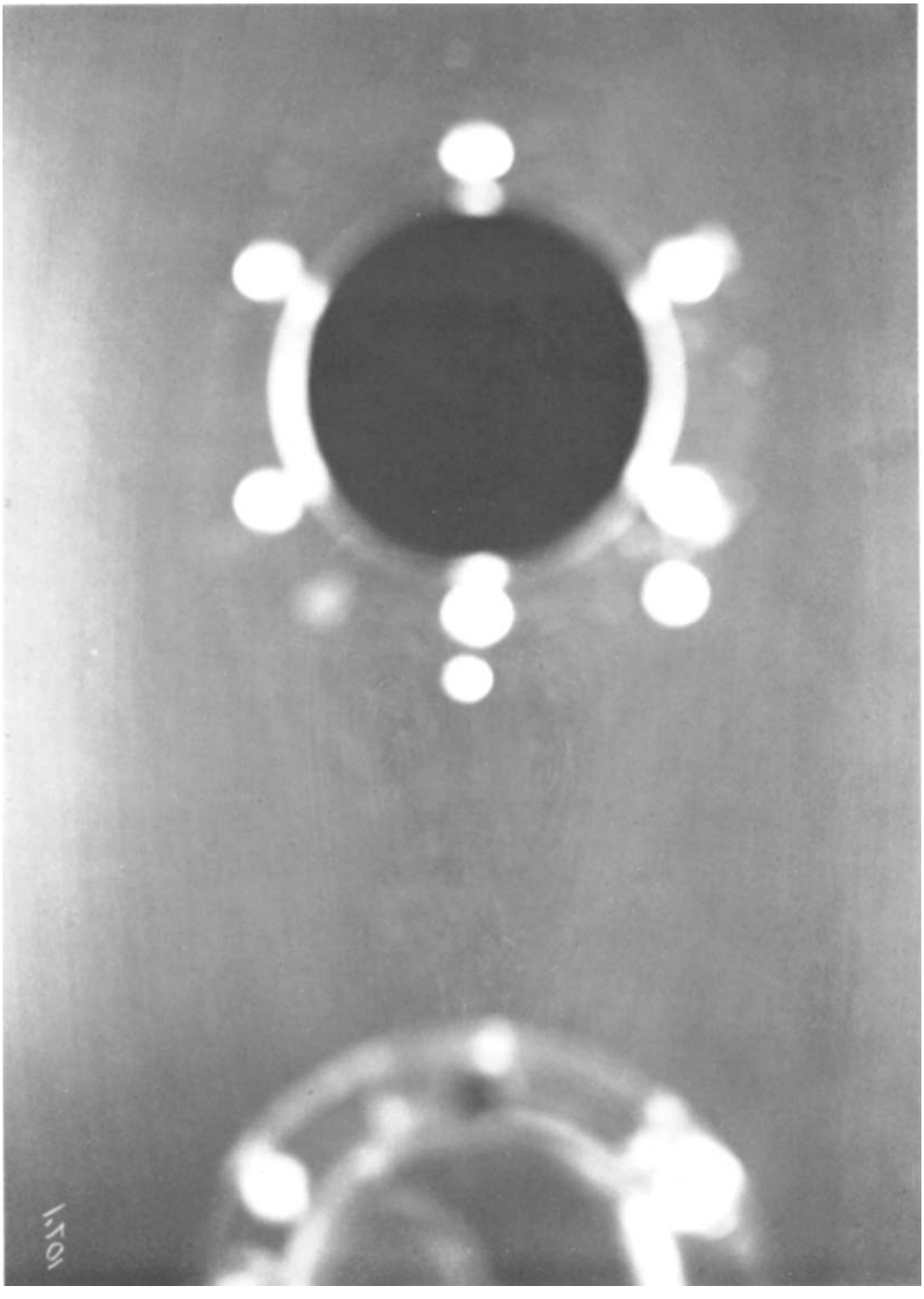

FIGURE 15. $R = 65$.

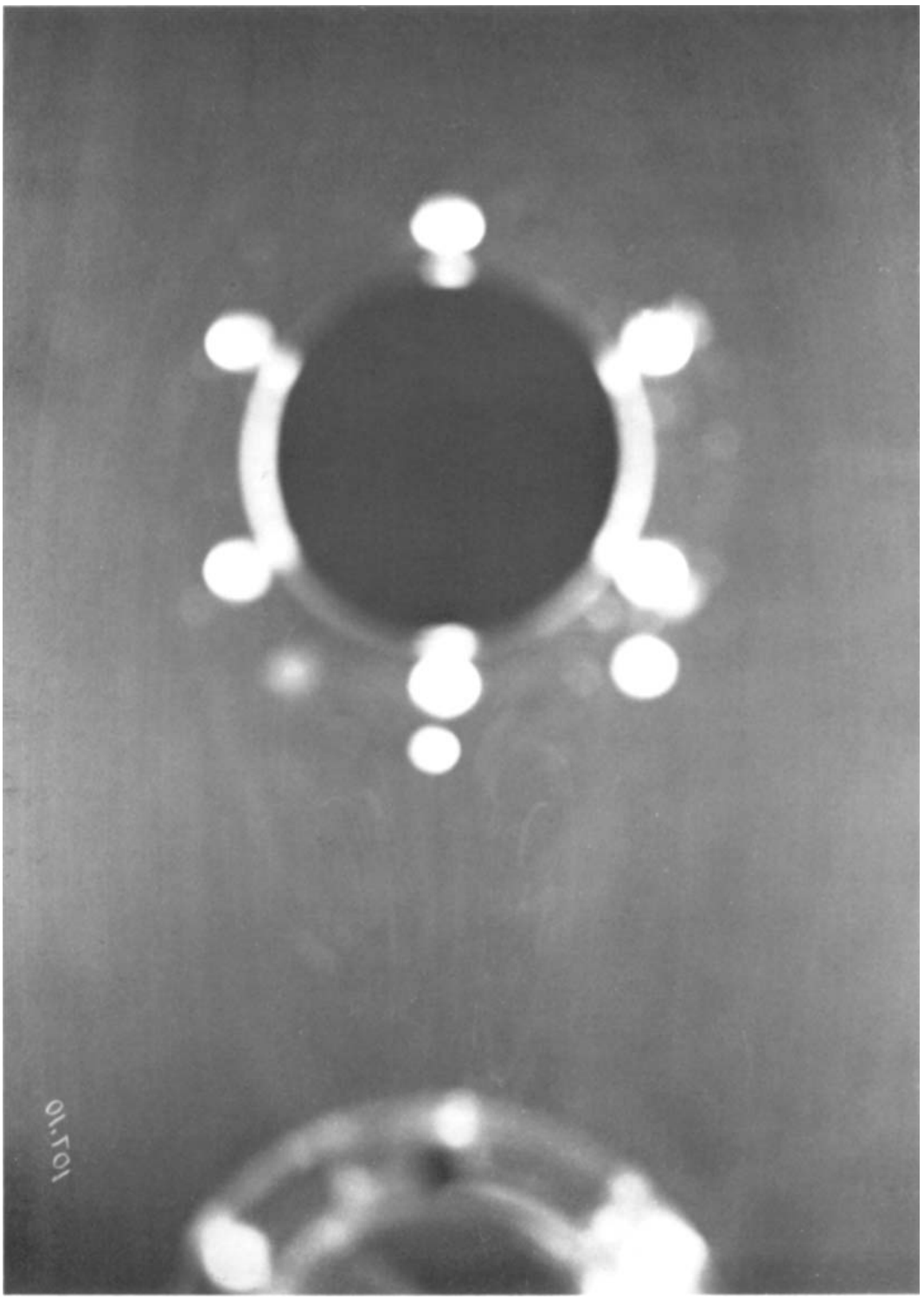

FIGURE 16. $R = 113$.

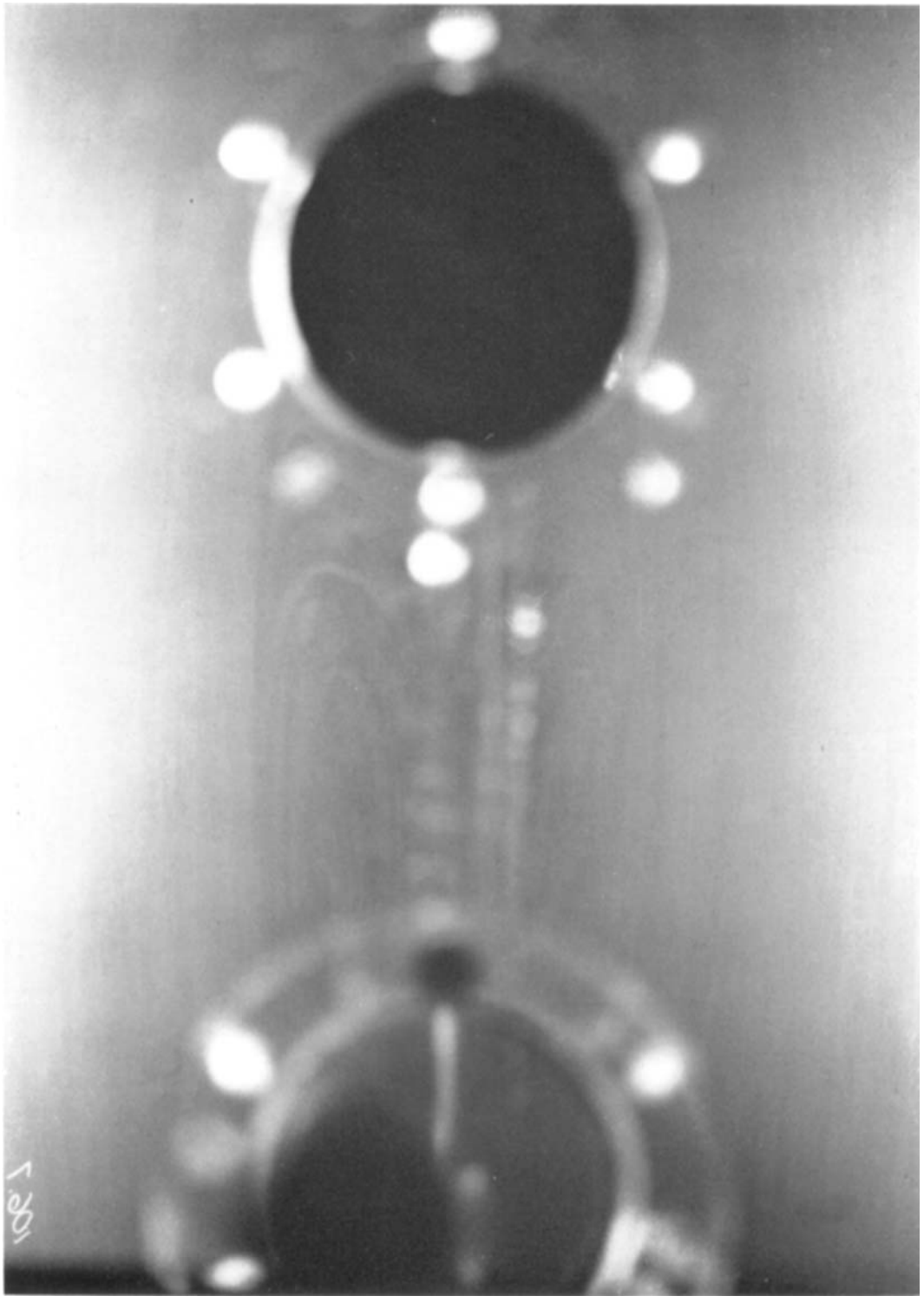

FIGURE 17. $R = 262$.